Available online at www.sciencedirect.com
SCIENCE DIRECT®
Polymer Degradation and Stability 91 (2006) 44–51
Polymer Degradation and Stability
www.elsevier.com/locate/polydegstab

Calorimetric and thermogravimetric studies of UV-irradiated polypropylene/starch-based materials aged in soil

J.M. Morancho [a,*], X. Ramis [a], X. Fernández [a], A. Cadenato [a], J.M. Salla [a], A. Vallés [b], L. Contat [b], A. Ribes [b]

[a] *Laboratori de Termodinàmica, ETS Enginyeria Industrial Barcelona, UPC, Av. Diagonal 647, 08028 Barcelona, Spain*
[b] *Departamento de Termodinámica, ETS Ingeniería Industrial Valencia, UPV, Camino de Vera s/n, 46022 Valencia, Spain*

Received 22 February 2005; received in revised form 21 April 2005; accepted 28 April 2005
Available online 1 July 2005

Abstract

We studied the biodegradability in soil of mixtures of polypropylene and a starch-based biodegradable additive. The changes in their properties were studied using calorimetry and thermogravimetric analysis. To observe the effect of UV radiation, the mixtures were photo-oxidized before biodegradation. The results were compared with those obtained from previous studies on non-photo-oxidized samples. Using calorimetry, we observed changes in the crystallinity of the samples and in their crystallization kinetics, which we analyzed using the Avrami equation. Photo-oxidation was found to reduce the crystallinity of the mixtures while degradation in soil increases it. Using thermogravimetry, we observed changes in the thermal stability and in the associated kinetic parameters, which we determined using an isoconversional integral method. Biodegradation tended to increase the thermal stability of the starch units and did not affect the polypropylene. Photo-oxidation tended to decrease the thermal stability of the mixture, although it may make the starch slightly more stable. The thermooxidative degradation of the mixtures was also studied.

Keywords: Biodegradation; Differential scanning calorimetry; Photo-oxidation; Thermal degradation

1. Introduction

Most synthetic polymers are resistant to environmental degradation and their useful lives tend to be short. These facts have led to a significant increase in the volume of residual plastics in recent years. One solution to this problem consists in making these materials degradable through the addition of biodegradable additives [1].

Polypropylene, like other polyolefins, is a non-biodegradable polymer, since micro-organisms are unable to metabolize it within an acceptable period of time. However, it is possible to endow it with a certain degree of biodegradability by adding polymers to it that are themselves easily degradable in nature, and which aid the break down of the polypropylene's molecular chains. Starch is normally added to polypropylene together with a pre-oxidant. To determine the useful lives of these materials it is necessary to know what changes their chemical and physical properties undergo during the degradation periods [2]. These changes are normally studied using conventional analytical techniques, such as differential scanning calorimetry (DSC) and thermogravimetric analysis (TGA) [3–6].

The mechanisms involved in the biodegradation of polyolefins are complex due to the interaction of different oxidative processes. These processes can be

* Corresponding author. Tel.: +34 934016531; fax: +34 934017389.
E-mail address: morancho@mmt.upc.edu (J.M. Morancho).

0141-3910/$ - see front matter © 2005 Elsevier Ltd. All rights reserved.
doi:10.1016/j.polymdegradstab.2005.04.029

caused by the oxygen present in the air, by microorganisms or by a combination of the two. Many other factors can influence biodegradation: UV radiation, photodegradable and biodegradable additives, the specific morphology involved, the surface area exposed, molecular weight, etc. [7,8].

For example, adding starch to low-density polyethylene increases its stability with regards to thermooxidation, but makes it less stable against UV radiation [9]. However, photo-oxidation increases the biodegradability of most polymers, since it breaks down their chains, which causes important changes in their properties [10,11].

The use of thermal analysis and mechanical spectroscopy to characterize the degradation of starch plastic composites has allowed us to observe that, although the degradation starts in the amorphous regions, the crystalline region is also affected by biodegradation in soil [12].

In this study, we used calorimetry and thermogravimetric analysis to study the accelerated degradation in soil of photo-oxidized mixtures of polypropylene and a commercially available starch-based additive, Mater-Bi AF05H. We compared our results with those obtained previously for the same mixtures when they were not subjected to photo-oxidation [13,14].

2. Theoretical analysis

2.1. Crystallization

Based on dynamic tests performed in the calorimeter, the total crystalline content, χ, was calculated using the equation:

$$\chi = \frac{(H_a - H_c)}{\Delta H_m} \tag{1}$$

where H_a and H_c are the enthalpies of the liquid state and the crystalline state, respectively. The difference between them is obtained directly from the thermogram by integrating the calorimetric signal. ΔH_m is the enthalpy of fusion of a perfect crystal of infinite size.

The crystallization kinetics was analyzed by means of the Avrami equation [15]:

$$X(t) = 1 - \exp(-Kt^n) \tag{2}$$

$$\ln(-\ln[1 - X(t)]) = n\ln t + \ln K \tag{3}$$

where $X(t)$ is the crystallized fraction or relative degree of crystallization, t is the time, n is the Avrami exponent and K is the constant of isothermal crystallization. For each crystallization temperature, the linear plot of $\ln(-\ln[1 - X(t)])$ against $\ln t$ allows n and $\ln K$ to be obtained from the slope and the intercept, respectively.

The crystallized fraction at a time t was calculated using the following equation:

$$X(t) = \frac{\Delta H_t}{\Delta H_{iso}} \tag{4}$$

where ΔH_t is the crystallization heat released before time t and ΔH_{iso} is the total isothermal crystallization heat. Both ΔH_t and ΔH_{iso} were obtained by integrating the calorimetric signal up to time t, and until the end of the exothermic peak, respectively.

The half crystallization time ($t_{1/2}$), defined as the time at which the degree of crystallization is 50%, was calculated from the Avrami equation (Eq. (2)) as:

$$t_{1/2} = \left(\frac{\ln 2}{K}\right)^{1/n} \tag{5}$$

The rate of crystallization was defined as the reciprocal of $t_{1/2}$:

$$\tau_{1/2} = \frac{1}{t_{1/2}} \tag{6}$$

In order to verify the calculated kinetic parameters, the experimental values of $t_{1/2}$ were compared with the values obtained from Eq. (5).

2.2. Thermal degradation

The rate of degradation or conversion, in thermogravimetric analysis, $d\alpha/dt$, can be defined as the rate of change of the degree of conversion. The degree of degradation or conversion is calculated in terms of mass loss as:

$$\alpha = \frac{w_o - w}{w_o - w_\infty} \tag{7}$$

where w_o, w and w_∞ are: the initial weight, the actual weight at each point of the curve, and the final weight measured at the end of the degradation process, respectively.

The kinetics of the degradation in non-isothermal conditions can be studied, using the Coats-Redfern approximation and taking that $2RT/E \ll 1$ [13,16], by means of:

$$\ln\frac{g(\alpha)}{T^2} = \ln\left[\frac{AR}{\beta E}\right] - \frac{E}{RT} \tag{8}$$

where $g(\alpha)$ is the integral conversion function, T is the absolute temperature, A is the pre-exponential factor, R is the gas constant, β is the heating rate and E is the activation energy. For a given kinetic model, plotting

$\ln[g(\alpha)/T^2]$ against $1/T$ allows us to determine E and A from the slope and the intercept.

Reordering Eq. (8) gives us:

$$\ln\frac{\beta}{T^2}=\ln\left[\frac{A\mathrm{R}}{g(\alpha)E}\right]-\frac{E}{\mathrm{R}T} \tag{9}$$

Plotting $\ln[\beta/T^2]$ against $1/T$ makes it possible to determine E and the kinetic parameter $\ln[A\mathrm{R}/g(\alpha)E]$ for every degree of conversion. This isoconversional procedure is equivalent to Kissinger's method [17] and similar to Ozawa's method [18,19].

If the degree of conversion at the peak does not vary with the rate of heating, Eq. (9) can be applied to the peak temperature, T_P, (maximum reaction rate):

$$\ln\frac{\beta}{T_\mathrm{P}^2}=\ln\left[\frac{A\mathrm{R}}{g(\alpha)E}\right]-\frac{E}{\mathrm{R}T_\mathrm{P}} \tag{10}$$

Once $g(\alpha)$ is known, plotting $\ln[\beta/T_\mathrm{P}^2]$ against $1/T_\mathrm{P}$ allows us to determine E and A [19].

In this study, we determined the complete kinetic triplet [E, A, $g(\alpha)$] associated with thermal degradation in a nitrogen atmosphere. Criado's reduced master curves procedure was used to determine the kinetic model [20]. The kinetic model which best describes the experimental data is the R_3 (surface-controlled reaction) model, with $f(\alpha)=3(1-\alpha)^{2/3}$ and $g(\alpha)=1-(1-\alpha)^{1/3}$. The activation energies and the parameters $\ln[A\mathrm{R}/g(\alpha)E]$ associated with the maxima of the thermogravimetric curves were calculated using Eq. (10). From these data, the pre-exponential factor for the R_3 model was calculated. Details of the method used are fully described in an earlier study [13].

3. Experimental

3.1. Materials

Polypropylene 1148-TC (PP) supplied by BASF (Germany) was blended with Mater-Bi AF05H supplied by Novamont North America (USA). PP incorporates a conventional thermal stabilizer of undisclosed composition. This stabilizer is a free radical scavenger that interferes with the degradation propagation reaction and limits heat damage caused by oxidation process. Mater-Bi AF05H is a starch-based additive that contains highly complex thermoplastic starch including ethylene–vinyl-alcohol copolymers (EVOH), with a starch content of nearly 50% by weight.

A homogeneous mixture with 50/50 PP/Mater-Bi AF05H by weight was initially prepared by melting in a Brabender Plasticorder PL 2100 rheometer. The blend was then cut as pellets and compression-moulded into rectangular bars (68 × 12 × 1.8 mm) using an M Carver press. This is the method followed in previous work [14,21].

The test samples were then photo-oxidized (using an Atlas Suntest) with ultraviolet radiation from a xenon lamp at solar radiation wavelengths. The total irradiation was 138 000 kJ/m^2 for a period of 98.7 h. The black body temperature was 53 °C. While the samples were exposed to the radiation, they were submerged in water which was pumped round in a closed circuit and maintained at 38 °C. They were then biodegraded in soil, and after different degradation times their crystallinity and thermal stability were studied using DSC and TGA, respectively.

3.2. Soil burial test

Soil burial tests were carried out according to the DIN 53739 international standard [22] over a period of one year. The soil used in these tests was a red soil extract taken from an agricultural field in Alginet (Valencia, Spain). The boxes were kept in a Hereaus B12 culture oven at a constant temperature of 28 ± 0.5 °C, and the pH and water content of the soil were controlled periodically. We measured the pH of a soil extract dissolved in distilled water, at a ratio of 1:20. The soil was maintained at approximately pH 7 and a relative humidity of 0.87 g water/g wet soil.

The samples were removed after different times: 20 days, 4 and 6 months. After removal, all the samples were carefully washed with a soap solution in order to stop the degradation, and they were blotted before analysis.

3.3. Differential scanning calorimetry (DSC)

A Mettler DSC30 calorimeter, connected to a TA4000 thermal analysis system, was used to measure crystallinity.

To determine the total crystalline content of the samples, a sequence of three dynamic scans was performed at 10 °C min^{-1}. During the first, the material was heated (25–200 °C) to melt it and completely erase its thermal history. It was then kept at 200 °C for 5 min. After that it was cooled to 25 °C in order to analyse the crystallization, and then the material was melted again (25–200 °C).

In order to study the isothermal crystallization kinetics, the samples were crystallized at 136 °C using the following sequence in the calorimeter: the sample was heated at 10 °C min^{-1} from 25 °C to 200 °C, kept in a molten state at 200 °C for 5 min, cooled at −80 °C min^{-1} from 200 °C to 136 °C, isothermal crystallization at 136 °C and finally heated from 120 °C to 200 °C at 10 °C min^{-1}, which causes fusion of the crystallized material.

3.4. Thermogravimetric analysis (TGA)

Thermogravimetric analysis was carried out in a Mettler TG50 thermobalance linked to a Mettler TA4000 analysis system. Non-isothermal degradations were carried out at heating rates of 1.5, 2.5, 5, 10 and 15 °C min^{-1}, between 25 °C and 600 °C, in nitrogen and oxygen atmospheres. The precision of reported temperatures was estimated to be ±2 °C. The mass of the samples was approximately 10 mg and the gas flow 200 cm^3 min^{-1} (measured under normal conditions).

4. Results and discussion

4.1. Crystallization

Figs. 1, 2 and 3 show the results of the dynamic tests performed in the calorimeter to determine crystallinity. The figures compare tests carried out on samples of photo-oxidized and biodegraded polypropylene/Mater-Bi, with those from a previous study [14] on the same type of samples subjected to the same biodegradation, but with no prior photo-oxidization. In Fig. 1, which corresponds to heating at 10 °C min^{-1}, the first fusion of different samples can be observed. Table 1 (first melting) gives the peak temperatures (T_m), the variation of enthalpy during fusion (Δh_m) and the total crystalline content (χ) (obtained using Eq. (1)) for photo-oxidized and biodegraded samples at different times. The peak temperature increases slightly with the time of biodegradation, while the other magnitudes show no overall tendency.

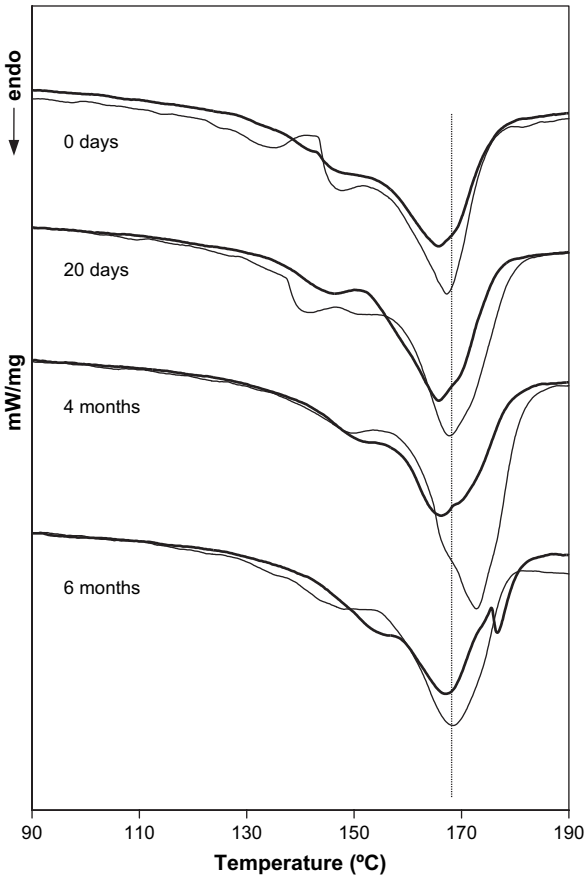

Fig. 1. First melting of the PP/Mater-Bi blend degraded in soil over different periods. The heavy lines represent the samples that were previously photo-oxidized, and the fine lines those that were not. The data for the non-photo-oxidized samples are from Cadenato et al. [14].

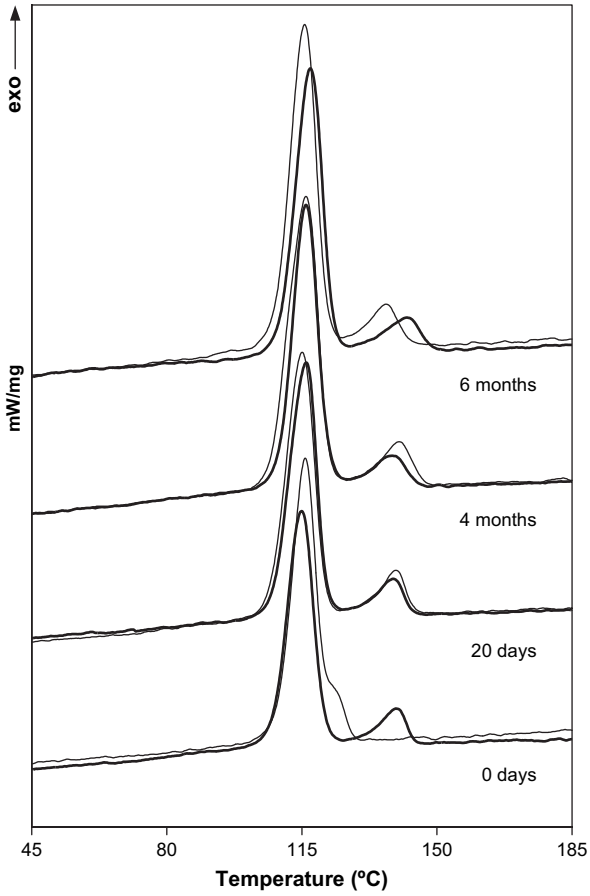

Fig. 2. Crystallization of the PP/Mater-Bi blend degraded in soil over different periods. The heavy lines represent the samples that were previously photo-oxidized and the fine lines those that were not. The data for the non-photo-oxidized samples are from Cadenato et al. [14].

Fig. 2 shows the cooling of the different samples at 10 °C min^{-1}, and the process of crystallization can be clearly seen. Table 1 (crystallization) gives the peak temperatures (T_c), the variation of enthalpy during crystallization (Δh_c) and the total crystalline content (χ). It can be seen that the enthalpy of crystallization and the crystallinity increase with the time of biodegradation and the peak crystallization temperature shows no overall tendency.

Fig. 3 shows the second fusion, achieved by reheating the sample at 10 °C min^{-1}. From Table 1 (second melting) it can be seen that the peak fusion temperature

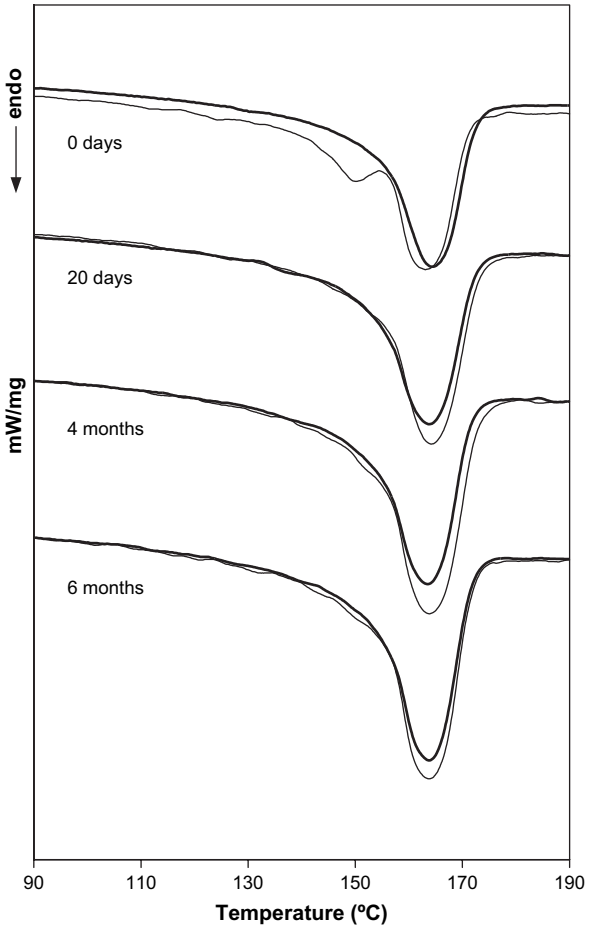

Fig. 3. Second melting of the PP/Mater-Bi blend degraded in soil over different periods. The heavy lines represent the samples that were previously photo-oxidized and the fine lines those that were not. The data for the non-photo-oxidized samples are from Cadenato et al. [14].

hardly changes, while the enthalpy of fusion and the crystallinity increase with the time of biodegradation. This is due to the fact that degradation is mainly taking place in the amorphous regions of the starch, which can increase crystallinity. If the data for crystallinity and the enthalpy of fusion from the two fusions are compared, it can be seen that they are lower in the second. This indicates that during the first fusion, when the thermal history of the material was erased, irreversible changes took place in the composite or that there are differences between the crystallization that takes place in the DSC and in the rheometer (where the samples were prepared initially).

Table 1 compares the data for the photo-oxidized samples with those for the non-photo-oxidized samples. It can be seen that the enthalpy of fusion and the total crystalline content are lower for the former. It could be the case that ultraviolet radiation leads to the formation of large quantities of radicals that increase the possibility of reactions between chains, thereby increasing the molecular weight of the polymer [9] and

Table 1
Calorimetric data for polypropylene/Mater-Bi blend which were photo-oxidized and biodegraded for different periods

Process	Time	T_m, T_c (°C)[a]	Δh_m, Δh_c (J/g)[a]	χ (%)[a,b]
1st Melting	0 days	166 (167)	84 (99)	44.8 (52.8)
	20 days	166 (168)	79 (96)	42.2 (51.1)
	4 months	167 (173)	84 (105)	45.0 (55.9)
	6 months	169 (168)	80 (103)	42.4 (54.9)
Crystallization	0 days	115 (116)	63 (64)	33.4 (34.1)
	20 days	117 (115)	67 (75)	35.7 (39.9)
	4 months	117 (116)	74 (85)	39.5 (45.3)
	6 months	117 (116)	79 (84)	42.0 (44.7)
2nd Melting	0 days	164 (163)	63 (70)	33.4 (37.3)
	20 days	164 (164)	69 (78)	36.7 (41.5)
	4 months	164 (164)	76 (89)	40.7 (42.4)
	6 months	164 (164)	76 (88)	40.4 (46.9)

[a] The data for the same samples without photo-oxidation are given in brackets. These data are from Cadenato et al. [14].
[b] Crystallinity was calculated using the heats of fusion of 100% crystalline materials. These heats were tentatively estimated based on the data for the additive contributions of groups [23], which are 207.2 J/g for polypropylene and 168.2 J/g for Mater-Bi.

therefore decreasing crystallinity. Although the peak fusion temperatures hardly change, the calorimetric data corresponding to the first melting (Fig. 1) show a different pattern. This suggests that during photo-oxidation certain changes are produced in the crystalline structure of the material that could be attributed to the existence of chain-elongation reactions after dominant chain-scission reactions [9].

Table 2 gives the results of isothermal crystallization. As the time of biodegradation increases, the kinetic parameter n in the Avrami equation (Eq. (2)) decreases, while the rate constant, K, increases. No significant changes are observed after the sixth month of biodegradation.

The changes in the value of the parameter n should be associated with a change in the microstructure of the material, since the thermal treatment is the same for all the systems studied. If this parameter takes the value 4, nucleation is homogeneous and crystalline growth is 3-dimensional. Values for n of 3 and 2 are associated with 3-dimensional and 2-dimensional growth with heterogeneous nucleation, respectively [24]. The decrease seen in n suggests a change from 3-dimensional to 2-dimensional growth.

Table 2
Avrami kinetic parameters obtained from crystallization tests at 136 °C on the PP/Mater-Bi blend which was photo-oxidized and biodegraded in soil for different periods

Degradation time	K (min^{-n})	n	$t_{1/2}$ (min)	$t_{1/2,\ exp}$ (min)	$\tau_{1/2}$ (min^{-1})
0 days	7.63×10^{-6}	3.2	36.2	35.5	0.0276
20 days	1.10×10^{-5}	3.2	31.6	30.8	0.0316
4 months	5.64×10^{-5}	2.8	29.6	28.3	0.0338
6 months	3.53×10^{-4}	2.3	27.5	26.6	0.0363

The increase in the value of the rate constant is associated with the fact that during biodegradation the polymer chains break down, and therefore crystallization takes place more quickly.

Table 2 also compares the experimental values of $t_{1/2}$ with those obtained by using Eq. (5). The similarity between the two demonstrates the strength of the methodology used and the accuracy of the kinetic parameters obtained (n and K). The rate of crystallization was calculated using Eq. (6).

The comparison between the data from the photo-oxidized samples and those from the non-photo-oxidized samples (obtained in a previous study [14]) shows that the former yield higher values of the parameter n, which would seem to indicate a more homogeneous system. Notwithstanding, the lower value of the rate constant for the photo-oxidized samples would indicate less, and slower, crystallization. All of this is consistent with the existence of chain-elongation reactions during photo-oxidation that give rise to materials with a greater molecular weight and which crystallize more homogeneously, but more slowly and to a lesser extent due to topological impediments.

4.2. Thermal degradation

In the experiments performed in the thermobalance (TGA), two stages were observed in the process of degradation of the photo-oxidized samples in nitrogen. The first corresponds to the degradation of the starch and the second to that of PP and EVOH together [13,25]. Fig. 4 shows the results obtained at a rate of 10 °C min^{-1}. The first stage can be seen to shift towards higher temperatures as the time of biodegradation increases. This indicates that the starch stabilizes during the process. This can also be seen in the values of the peak temperatures given in Table 3, which increase as the time of biodegradation increases. In contrast, the second stage hardly varies at all, as can be seen in both Fig. 4 and in the peak temperatures in Table 3.

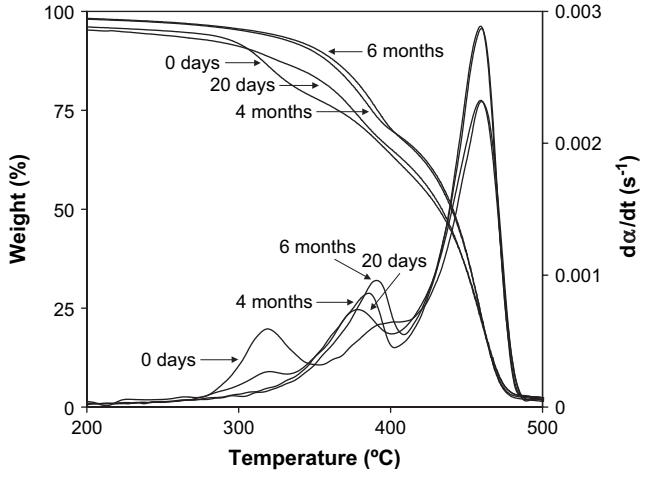

Fig. 4. Thermogravimetric analysis (percentage of residual weight and change in the degree of conversion with time) at 10 °C min^{-1} in a nitrogen atmosphere for a PP/Mater-Bi blend photo-oxidized and degraded in soil over different periods.

Fig. 5 shows the degree of degradation and the rate of degradation plotted against temperature in nitrogen at different heating rates, for a PP/Mater-Bi sample which was photo-oxidized and biodegraded in soil for 4 months. Similar curves were obtained for the other mixtures studied (these are not included). It can be seen that as the rate of heating is increased, the curves shift to higher temperatures and the rate of thermal degradation increases.

The value of the kinetic parameters (activation energy and frequency factor) given in Table 3 were obtained by applying Eq. (10) to the maxima of the $d\alpha/dt - T$ curves and assuming an R_3 mechanism. The reduced master curves $f(\alpha)g(\alpha) - \alpha$ [20] show that this was the most suitable mechanism for describing the two thermal degradation processes in these samples. Due to the overlapping of the degradation processes, it was necessary to deconvolute the $d\alpha/dt - T$ curves to establish that the best kinetic model is the R_3 model. This procedure was also followed in a previous study [13]. Due to the compensation effect that exists between the activation energy and the frequency factor [26,27], we also obtained, as a comparative parameter, the rate constant at 400 °C from the Arrhenius equation. As before, one can see that in the first stage the results are different when the sample has not been biodegraded, while in the second stage there are no significant differences. During biodegradation, the stability of the material increases due to degradation in the amorphous parts of the starch. This allows it to recrystallize, and this is why the rate constant increases with the biodegradation time. Using long biodegradation times, there is a certain difference between the values of the activation energy in the first stage, but the difference that also exists in the pre-exponential factor counteracts this change and therefore the rate constant calculated at 400 °C is similar. This effect also occurs in the kinetic parameters for the second stage when the degradation rates are almost equal for all the different times.

The thermogravimetric curves and the kinetic parameters associated with them for similar samples that did not undergo photo-oxidation can be found in a previous study [13]. These parameters were also obtained from Eq. (10) and under the assumption of an R_3 mechanism. Comparing the previous results with those of the photo-oxidized samples, it can be seen that both groups of samples undergo thermal degradation in a similar way, although the thermogravimetric curves for the photo-oxidized materials are shifted to slightly lower temperatures. This indicates that the process of photo-oxidation tends to reduce the overall thermal stability of these

Table 3
Kinetic parameters for the thermal degradation process in a nitrogen atmosphere of samples which were photo-oxidized and biodegraded in soil for different periods

Time	1st Step[a]				2nd Step[a]			
	T_P[b] (°C)	E (kJ mol^{-1})	ln A (min^{-1})	k_{400}[c] (min^{-1})	T_P[b] (°C)	E (kJ mol^{-1})	ln A (min^{-1})	k_{400}[c] (min^{-1})
0 days	319	180	34.3	8.45	459	153	23.0	0.0135
20 days	380	149	24.9	0.171	459	151	22.7	0.0135
4 months	384	135	22.3	0.163	457	167	25.5	0.0127
6 months	391	135	22.4	0.171	459	147	22.1	0.0150

[a] The two stages of decomposition are referred to as 1 and 2 in order of increasing temperature. The first stage corresponds to decomposition of the starch of Mater-Bi and the second to the decomposition of the PP and the EVOH of Mater-Bi together.
[b] T_P is the peak temperature of the $d\alpha/dt - T$ curve at a rate of 10 °C min^{-1}.
[c] In order to compare the results of the degraded samples, the rate constant was calculated at 400 °C, k_{400}, from the values of E and ln A using the Arrhenius equation.

materials. Probably during irradiation the antioxidants have been destroyed and the sample filled with peroxides. A more detailed analysis based on the kinetic parameters shows that although the rate constants are similar in the photo-oxidized and the non-photo-oxidized samples, the non-photo-oxidized samples have values of k that are lower in the second stage and higher in the first. This would seem to indicate that the photo-oxidation tends mainly to destabilize PP and EVOH, but it could even stabilize starch to a slight degree. The mixture that was degraded for 20 days behaves slightly differently in the two treatments carried out. When this sample is photo-oxidized, the thermal stability of the first stage increases considerably and the peak appears at a much higher temperature. Furthermore, k is much lower than for the non-photo-oxidized sample.

Fig. 6 shows the results of the thermogravimetric test carried out in an oxygen atmosphere at 10 °C min^{-1}. In general, the weight loss takes place in two stages that are not related to the composition of the mixtures but rather to oxidative processes that take place during the test. The presence of oxygen means that weight loss starts about 100 °C below the temperature at which it started in the nitrogen atmosphere (see Fig. 5). The photo-oxidized sample that has not undergone biodegradation starts to decompose first. However, if it is subjected to biodegradation, it stabilizes and decomposes in a similar way as the sample that was not photo-oxidized, but which was subjected to the same time of biodegradation. For all the samples except the non-photo-oxidized and non-biodegraded sample, there is a temperature above which the degradation rate decreases and then later, at above 400 °C, it increases again. This may be due to the formation of a more stable substance during oxidation in the thermobalance, which does not start to decompose until high temperatures are reached. The photo-oxidized and non-biodegraded sample starts to decompose first and is the one which completes

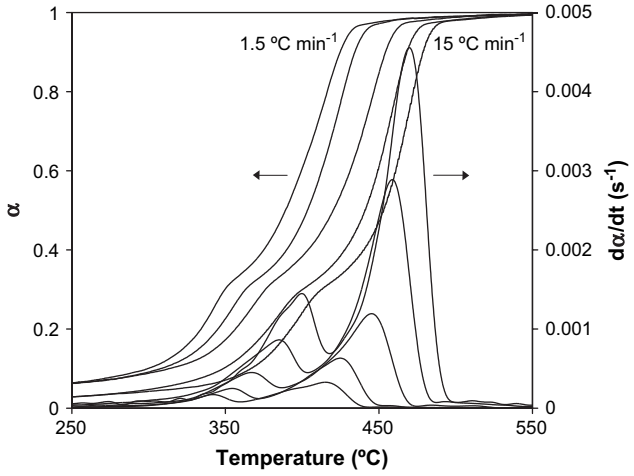

Fig. 5. Thermogravimetric analysis (degree of conversion and change in the degree of conversion with time) at different rates of heating in a nitrogen atmosphere for a PP/Mater-Bi blend photo-oxidized and degraded in soil over 4 months. Heating rates: 1.5, 2.5, 5, 10, 15 °C min^{-1}.

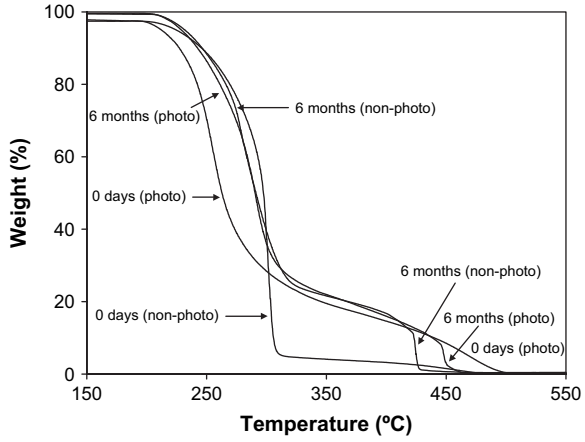

Fig. 6. Thermogravimetric analysis (percentage of residual weight) at 10 °C min^{-1} in an oxygen atmosphere for a PP/Mater-Bi blend degraded in soil over different periods. Some samples were photo-oxidized previously (photo) and others were not (non-photo). The non-photo-oxidized data are from Ramis et al. [13].

degradation at the highest temperature, possibly due to the combined effect of photo-oxidation and later oxidation in the thermobalance in an oxygen atmosphere.

5. Conclusions

Using calorimetry and thermogravimetric analysis we have shown that biodegradation in soil and UV radiation modify the properties of mixtures of PP and Mater-Bi.

The rate of crystallization and the Avrami exponent reflect the influence of the processes of photo-oxidation and degradation in soil on crystallization. Therefore, these can be used as comparative parameters in these processes. The increase in crystallinity during biodegradation in soil is attributed to the breaking down of chains that exist in the amorphous regions of the starch, which thus allows recrystallization. Tentatively, we have attributed the reduction in crystallinity observed during photo-oxidation to the formation of free radicals that would favour chain-elongation reactions.

The changes that the different components of the PP/Mater-Bi mixtures undergo during biodegradation and photo-oxidation are evident from their thermal stability and the kinetic parameters associated with their thermal degradation. Biodegradation mainly affects the starch, whose thermal stability increases, and has no significant effect on the PP or the EVOH. Photo-oxidation decreases the overall stability of the mixture, although it may slightly stabilize the starch.

The thermooxidative degradation of the PP/Mater-Bi mixtures is complex due to the combined action of the oxidative processes that are present during photo-oxidation and/or biodegradation, and the oxidation that takes place in the thermobalance. In an oxygen atmosphere the mixtures break down into two distinct stages; there is also an intermediate stage characterized by a very slow rate of degradation. The second stage is attributed to the formation of more stable species during oxidation, which do not break down until high temperatures are reached. These species could form during photo-oxidation, biodegradation or during thermooxidative testing.

Acknowledgements

This work was supported by CICYT and FEDER through Grants PPQ2001-2764-C03-02, PPQ2001-2764-C03-01 and MAT2004-04165-C02-02.

References

[1] Griffin GJL, editor. Chemistry and technology of biodegradable polymers. Glasgow: Blackie; 1994.
[2] Navarro R, Torre L, Kenny JM, Jiménez A. Polym Degrad Stab 2003;82:279–90.
[3] Bockhorn H, Hornung A, Hornung U, Shawaller D. J Anal Appl Pyrol 1999;48:93–109.
[4] Ceamanos J, Mastral JF, Millera A, Aldea ME. J Anal Appl Pyrol 2002;65:93–110.
[5] Gao Z, Amasaki I, Nakada M. J Anal Appl Pyrol 2003;67:1–9.
[6] Gao Z, Taneko T, Amasaki I, Nakada M. Polym Degrad Stab 2003;80:269–74.
[7] Albertsson AC, Andersson SV, Karlsson S. Prog Polym Sci 1987;18:73–87.
[8] Albertsson AC, Karlsson S. Prog Polym Sci 1990;15:177–92.
[9] Erlandsson B, Karlsson S, Albertsson AC. Polym Degrad Stab 1997;55:237–45.
[10] Pandey JK, Singh RP. Biomacromolecules 2001;2:880–5.
[11] Feldman D. J Polym Environ 2002;10:163–73.
[12] Contat-Rodrigo L, Ribes-Greus A. Macromol Symp 1999;144:153–63.
[13] Ramis X, Cadenato A, Salla JM, Morancho JM, Vallés A, Contat L, et al. Polym Degrad Stab 2004;86:483–91.
[14] Cadenato A, Ramis X, Salla JM, Morancho JM, Contat L, Ribes A, et al., J Appl Polym Sci, in press.
[15] Avrami M. J Chem Phys 1939;7:1103–12.
[16] Coats AW, Redfern JP. Nature 1964;201:68–9.
[17] Kissinger HE. Anal Chem 1957;24:1702–6.
[18] Ozawa T. Bull Chem Soc Jpn 1965;1881–6.
[19] Salla JM, Morancho JM, Cadenato A, Ramis X. J Therm Anal Cal 2003;72:719–28.
[20] Criado JM. Thermochim Acta 1978;24:186–9.
[21] Contat-Rodrigo L, Ribes-Greus A, Díaz-Calleja R. J Appl Polym Sci 2001;82:2174–84.
[22] DIN 53739 International Norm, November 1984.
[23] van Krevelen DW. Properties of polymers. 3rd ed. Amsterdam: Elsevier; 1994.
[24] Sesták J. In: Svehla G, editor. Thermophysical properties of solids. Comprehensive analytical chemistry. Thermal analysis, vol. XII. Amsterdam: Elsevier; 1984, p. 212.
[25] Wang XL, Yang KK, Wang YZ, Wu B, Liu Y, Tang B. Polym Degrad Stab 2003;81:415–21.
[26] Ramis X, Salla JM, Cadenato A, Morancho JM. J Therm Anal Cal 2003;72:707–18.
[27] Vyazovkin S, Linert W. Int Rev Phys Chem 1995;14:355.